**RAA 2018** Vol. **18** No. **4**, 38(8pp) doi: 10.1088/1674–4527/18/4/38

*http://www.raa-journal.org* *http://iopscience.iop.org/raa*

***R**esearch in*
***A**stronomy and*
***A**strophysics*

# A model of Saturn inferred from its measured gravitational field

Dali Kong[1,2], Keke Zhang[2,3], Gerald Schubert[4] and John D. Anderson[5]

[1] Key Laboratory of Planetary Sciences, Shanghai Astronomical Observatory, Chinese Academy of Sciences, Shanghai 200030, China
[2] College of Engineering, Mathematics and Physical Sciences, University of Exeter, Exeter, EX4 4QF, UK
[3] Lunar and Planetary Science Laboratory, Macau University of Science and Technology, Macau, China; *kzhang@ex.ac.uk*
[4] Department of Earth, Planetary and Space Sciences, University of California, Los Angeles, CA 90095-1567, USA
[5] Jet Propulsion Laboratory, 4800 Oak Grove Drive, Pasadena, CA 91109, USA

Received 2017 December 19; accepted 2018 February 6

**Abstract** We present an interior model of Saturn with an ice-rock core, a metallic region, an outer molecular envelope and a thin transition layer between the metallic and molecular regions. The shape of Saturn's 1 bar surface is irregular and determined fully self-consistently by the required equilibrium condition. While the ice-rock core is assumed to have a uniform density, three different equations of state are adopted for the metallic, molecular and transition regions. The Saturnian model is constrained by its known mass, its known equatorial and polar radii, and its known zonal gravitational coefficients, $J_{2n}, n = 1, 2, 3$. The model produces an ice-rock core with equatorial radius $0.203\,R_{\rm S}$, where $R_{\rm S}$ is the equatorial radius of Saturn at the 1-bar pressure surface; the core density $\rho_{\rm c} = 10388.1\,{\rm kg\,m^{-3}}$ corresponding to 13.06 Earth masses; and an analytical expression describing the Saturnian irregular shape of the 1-bar pressure level. The model also predicts the values of the higher-order gravitational coefficients, $J_8, J_{10}$ and $J_{12}$, for the hydrostatic Saturn and suggests that Saturn's convective dynamo operates in the metallic region approximately defined by $0.2\,R_{\rm S} < r_{\rm e} < 0.7\,R_{\rm S}$, where $r_{\rm e}$ denotes the equatorial radial distance from the Saturnian center of figure.

**Key words:** gravitation — planets and satellites: individual (Saturn) — planets and satellites: interiors

## 1 INTRODUCTION

The existing interior models of Saturn (see, for example, Hubbard 1973; Stevenson 1982; Guillot 2005) suggest that its interior consists mainly of a central ice-rock core, a metallic electrically conducting dynamo region, an outer molecular envelope where its fast zonal winds might originate and an abrupt or a gradual transition between the metallic and molecular regions. However, the size of the inner core, the location of the Saturnian dynamo and the depth of the zonal winds are unknown. The high-precision gravitational field measurements anticipated from the Cassini Grand Finale offer a means of probing the internal structure of Saturn. However, the construction of an accurate Saturnian model enabling that interpretation represents a major challenge. This paper presents the first self-consistent, four-layer Saturn model that, constrained by its known mass, its known equatorial/polar radii and its known low-order zonal gravitational coefficients $J_{2n}, n = 1, 2, 3$, provides the irregular shapes of its 1-bar surface and all its internal interfaces, the size and density of its ice-rock core, the location of its convective dynamo and the values of its higher-order gravitational coefficients $J_8, J_{10}, J_{12}$.

There are at least two uncertainties in constructing any interior model of Saturn: its rotation period and its equation of state (EOS), i.e., the relationship between pressure $p$ and density $\rho$, denoted by $p = f(\rho)$. Since Saturn's rotation axis almost aligns with its magnetic pole, its internal rotation rate cannot be accurately deter-

mined from the observed magnetic data. The radio measurements from the Voyager spacecraft estimated a period of 10 h 39 min 22.4 s (Smith et al. 1982); Anderson & Schubert (2007), using the Cassini spacecraft data together with Pioneer and Voyager data, suggested a period of 10 h 32 min 35±13 s; Helled et al. (2015), based on an optimization approach using the gravitational field and shape of Saturn, obtained a period of 10 h 32 min 45±46 s; and Read et al. (2009) derived a period of 10 h 34 min 13±20 s based on the analysis of Saturn's atmospheric potential vorticity. The rotation period of Helled et al. (2015) will be adopted in our Saturnian model.

Three different types of EOS have been employed in previous studies: a physical EOS (see, for example, Saumon et al. 1995; Militzer 2013), an empirical EOS (see, for example, Anderson & Schubert 2007; Helled et al. 2015) and the classic polytropic EOS (see, for example, Chandrasekhar 1933; Hubbard 1999; Horedt 2004; Cao & Stevenson 2017). In the polytropic EOS, the density of a compressible barotropic fluid is a function only of the pressure $p$ described by the polytropic law, $p = f(\rho) = K\ \rho^{1+1/n}$, where $n$ is an integer and $K$ is assumed to be a constant. While the polytropic index of unity with $n = 1$ is believed to provide a reasonably good approximation for Jupiter's interior (see, for example, Hubbard 1999; Kong et al. 2013), the value of the index for Saturn is thought to be slightly different from unity (see, for example, Horedt 2004). We shall adopt the polytropic EOS in this study although the method and approach can be readily extended to other forms of the EOS. There are also significant uncertainties in the physical EOS for Saturn which may result from the location of the helium-poor to helium-rich region and the unknown helium to hydrogen ratio (see, for example, Guillot 2005). We shall regard the mass $M_{\rm S}$, the rotation rate $\Omega_{\rm S}$, the equatorial radius $R_{\rm S}$ and the polar radius $R_{\rm p}$ of Saturn as the known parameters in our Saturnian model.

The Saturnian gravitational field is intimately connected with its shape, described by its irregular surface $\mathcal{S}_{\rm o}$ at the 1-bar pressure level and its interior density distribution $\rho(\boldsymbol{r})$, where $\boldsymbol{r}$ is the position vector with the origin at the center of figure of the planet. The external gravitational field of Saturn can be conveniently described by the potential $V_{\rm g}(\boldsymbol{r})$

$$V_{\rm g}(\boldsymbol{r}) = -\frac{GM_{\rm S}}{r}\left\{1 - \sum_{n=1}^{\infty} J_{2n}\left(\frac{R_{\rm S}}{r}\right)^{2n} P_{2n}(\cos\theta)\right\}, \tag{1}$$

where $(r, \theta, \phi)$ are spherical polar coordinates with the corresponding unit vectors $(\hat{\boldsymbol{r}}, \hat{\boldsymbol{\theta}}, \hat{\boldsymbol{\phi}})$ and $\theta = 0$ being at the axis of rotation, $|\boldsymbol{r}| = r > R_{\rm S}$, $P_{2n}(\cos\theta)$ denotes the Legendre functions, $G$ is the universal gravitational constant ($G = 6.673848 \times 10^{-11}\,{\rm m^3\,kg^{-1}\,s^{-2}}$), $n$ takes integer values and $J_{2n}$ are the zonal gravitational coefficients. While the first three zonal gravitational coefficients $J_2, J_4, J_6$ are already accurately measured (see, for example, Helled et al. 2015), the high-precision measurements carried out by the Cassini Grand Finale are likely to determine the higher-order gravitational coefficients with $n \geq 8$.

Saturn departs more substantially from spherical geometry than Jupiter: the eccentricity at the one-bar surface is $\mathcal{E}_J = 0.3543$ for Jupiter while it is $\mathcal{E}_{\rm S} = 0.4316$ for Saturn (Seidelmann et al. 2007). Classical perturbation theories (Zharkov & Trubitsyn 1978) are based on a perturbation expansion around spherical geometry using a small rotation parameter $q = \Omega_{\rm S}^2 \bar{R}_{\rm S}^3/(GM_{\rm S})$, where $\bar{R}_{\rm S}$ denotes the mean radius of Saturn. In the perturbation analysis, for instance, the widely used third-order theory (see, for example, Anderson & Schubert 2007) expands $J_2$ in terms of the small parameter $q$ in the form

$$J_2 = C_1 q + C_2 q^2 + C_3 q^3,$$

where the expansion coefficients $C_1, C_2$ and $C_3$ are determined by the internal density $\rho(\bar{r})$ described by the hydrostatic equilibrium equation

$$\frac{1}{\rho(\bar{r})}\frac{{\rm d}p(\bar{r})}{{\rm d}\bar{r}} = -\frac{G\overline{M}_{\rm S}(\bar{r})}{\bar{r}^2} + \frac{2}{3}\Omega_{\rm S}^2\bar{r}, \tag{2}$$

where $\bar{r}$ denotes the mean radius distance and $\overline{M}_{\rm S}(\bar{r})$ is the mass enclosed by the spherical surface with radius $\bar{r}$. Although classical perturbation theories are mathematically simple, they require an unpractically large number of terms in the expansion to reach the high precision needed for the anticipated observations of Saturn's gravitational field by Cassini. It is therefore necessary to take a more accurate approach – computing the exact solution of Saturn without making any geometrical approximations – in order to interpret the high-precision gravitational measurements for Saturn.

We shall present a geometrically exact, physically realistic and computationally accurate model of Saturn. In this model, the spheroidal-shape approximation (Kong et al. 2013) – which assumes the outer bounding surface of a giant planet is in the shape of an oblate spheroid – is completely removed; Saturn's shape is *irregular* and

determined fully self-consistently by the required equilibrium condition; an ice-rock core is introduced and its non-spherical shape and its density are determined self-consistently as part of the coupled, multi-layered system; and a thin transition layer between the metallic and molecular regions is also introduced. Constrained by the known mass $M_{\rm S}$, the known equatorial radius $R_{\rm S}$ and the known polar radius $R_{\rm p}$, and the known zonal gravitational coefficients, $J_{2n}, n = 1, 2, 3$ of Saturn, our study is able to determine the shape and size of the ice-rock core, the irregular shape of Saturn at the 1-bar pressure level, to predict the values of higher-order gravitational coefficients, $J_8, J_{10}, J_{12}$; and to suggest the region where Saturn's convective dynamo is operating.

In what follows we begin by presenting the exact model of Saturn and the governing equations in Section 2, followed by discussion of the results in Section 3 with a summary and some remarks given in Section 4.

## 2 MODEL AND METHOD

Similar to existing Saturnian models (see, for example, Stevenson 1982; Guillot 2005), our multi-layer model of Saturn consists of three major parts: an ice-rock inner core, a metallic region where the Saturnian magnetic field is generated by its convective dynamo and an outer molecular insulating envelope where the observed cloud-level zonal winds might originate. A sketch of the multi-layered Saturnian model is given in Figure 1. Our Saturnian model is geometrically marked by the four irregular but axially symmetric surfaces: the core–metallic interface $\mathcal{S}_{\rm c}$, the metallic–transition interface $\mathcal{S}_{\rm t}$, the transition–molecular interface $\mathcal{S}_{\rm m}$ and the outer 1-bar-pressure surface $\mathcal{S}_{\rm o}$, all depicted in Figure 1. All four surfaces are geometrically irregular and determined fully self-consistently as a coupled hydrostatic system. For the convenience of discussion, the region surrounded by $\mathcal{S}_{\rm c}$ is denoted by $\mathcal{D}_{\rm c}$, the domain enclosed between $\mathcal{S}_{\rm m}$ and $\mathcal{S}_{\rm o}$ is denoted by $\mathcal{D}_{\rm m}$ and the domain enclosed between $\mathcal{S}_{\rm c}$ and $\mathcal{S}_{\rm o}$ is denoted by $\mathcal{D}_{\rm o}$.

In our Saturnian model, the density $\rho_1(\boldsymbol{r})$ of the fully compressible fluid exterior to the ice-rock core in the metallic region is assumed to be a function only of the pressure $p_1(\boldsymbol{r})$ obeying the polytropic law

$$p_1(\boldsymbol{r}) = K_1 \left[\rho_1(\boldsymbol{r})\right]^{1+1/n_1}, \tag{3}$$

where both $K_1$ and $n_1$ are constant; the density $\rho_2$ of the fluid in the outer molecular region is also assumed to obey a similar polytropic law,

$$p_2(\boldsymbol{r}) = K_2 \left[\rho_2(\boldsymbol{r})\right]^{1+1/n_2}, \tag{4}$$

but $K_2$ and $n_2$ are different constants; between the metallic and molecular regions the values of $K$ and $n$ are assumed to vary across the transition layer. In other words, three different polytropic laws are employed for the metallic region, the transition layer and the molecular region respectively which are marked by different physical properties (see, for example, Stevenson 1982).

Our Saturnian model further assumes that contributions from the mass beyond the 1-bar pressure surface $\mathcal{S}_{\rm o}$ are negligibly small and that Saturn is isolated and rotating rapidly with a uniform angular velocity $\hat{\boldsymbol{z}}\Omega_{\rm S}$. The above assumptions lead to the following governing equations for the fluid region $\mathcal{D}_{\rm o}$ of Saturn

$$0 = -\tfrac{1}{\rho(\boldsymbol{r})}\nabla p(\boldsymbol{r}) - \nabla V_{\rm g}(\boldsymbol{r}) - \tfrac{\Omega_{\rm S}^2}{2}\nabla|\hat{\boldsymbol{z}}\times\boldsymbol{r}|^2, \tag{5}$$

$$p(\boldsymbol{r}) \;=\; K(\boldsymbol{r})\rho(\boldsymbol{r})^{1+\frac{1}{n(\boldsymbol{r})}}, \tag{6}$$

$$\nabla^2 V_{\rm g}(\boldsymbol{r}) \;=\; 4\pi G\rho(\boldsymbol{r}), \tag{7}$$

where $K(\boldsymbol{r})$ and $n(\boldsymbol{r})$ mean that they are functions of $\boldsymbol{r}$ in the fluid region $\mathcal{D}_{\rm o}$, $p(\boldsymbol{r})$ is the pressure and $\rho(\boldsymbol{r})$ is the density, and $V_{\rm g}(\boldsymbol{r})$ is the gravitational potential. Equations (5)–(7) are solved subject to the two boundary conditions at the 1-bar pressure surface $\mathcal{S}_{\rm o}$

$$[p]_{|\boldsymbol{r}|=\mathcal{S}_{\rm o}} = 1\,\text{bar}, \tag{8}$$

$$G\left[\iiint_{\mathcal{D}_{\rm c}} \frac{\rho_{\rm c}\,{\rm d}^3\boldsymbol{r}'}{|\boldsymbol{r}-\boldsymbol{r}'|} + \iiint_{\mathcal{D}_{\rm o}} \frac{\rho\,(\boldsymbol{r}')\;{\rm d}^3\boldsymbol{r}'}{|\boldsymbol{r}-\boldsymbol{r}'|} + \frac{\Omega_{\rm S}^2}{2}\,|\hat{\boldsymbol{z}}\times\boldsymbol{r}|^2\right]_{|\boldsymbol{r}|=\mathcal{S}_{\rm o}} = \text{cons.}, \tag{9}$$

where $[\mathcal{F}]_{|\boldsymbol{r}|=\mathcal{S}_{\rm o}}$ denotes the evaluation of a function $\mathcal{F}$ at the 1-bar pressure surface $\mathcal{S}_{\rm o}$ that is *not only irregular but also a priori unknown*, Equation (9) requires the surface $\mathcal{S}_{\rm o}$ to be equipotential and $\iiint_{\mathcal{D}}\,{\rm d}^3\boldsymbol{r}'$ represents the volume integration over the domain $\mathcal{D}$.

The governing Equations (5)–(7), subject to the hydrostatic equilibrium conditions (8)–(9), are solved using a three-dimensional finite element method by making a three-dimensional tetrahedralization of the irregular solution domain that produces a finite element mesh without pole or central numerical singularities (Kong et al. 2016). For the results reported in this paper, the irregular solution domain of Saturn is typically divided into about $10^7$ tetrahedral elements to ensure the accuracy of the numerical solutions.

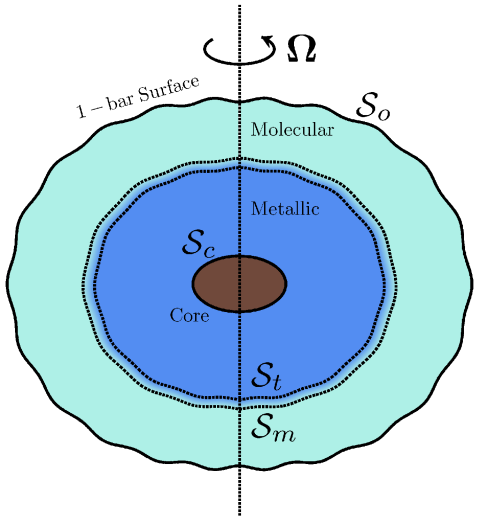


**Fig. 1** Sketch of the four-layer Saturnian model in a meridional plane: an ice-rock core, a metallic hydrogen-helium dynamo region, an outer molecular insulating envelope and a thin metallic–molecular transition layer. Four *geometrically irregular* surfaces characterize the model: the core-metallic interface $\mathcal{S}_{\rm c}$, the metallic-transition interface $\mathcal{S}_{\rm t}$, the transition-molecular interface $\mathcal{S}_{\rm m}$ and the outer 1-bar-pressure surface $\mathcal{S}_{\rm o}$.

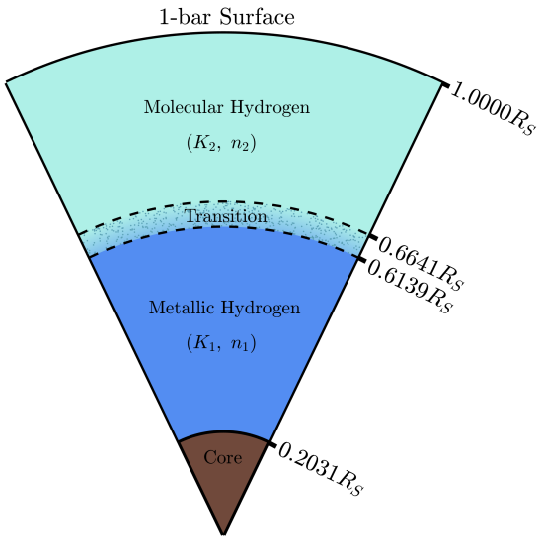


**Fig. 2** The Saturnian interior structure in the equatorial plane resulting from our exact model. In addition to the location of the three interfaces $\mathcal{S}_{\rm c}$, $\mathcal{S}_{\rm t}$ and $\mathcal{S}_{\rm m}$, it also gives an ice-rock core with the equatorial radius $0.2031\ R_{\rm S}$ and density $\rho_{\rm c} = 10388.1\,{\rm kg\,m^{-3}}$ corresponding to 13.06 Earth masses.

## 3 RESULTS AND DISCUSSIONS

The values of mass $M_{\rm S}$, equatorial radius $R_{\rm S}$, polar radius $R_{\rm p}$ and angular velocity $\Omega_{\rm S}$ used in our Saturnian model are listed in Table 1. With these four known parameters of Saturn, together with an initial guess for the core properties, for the three polytropic laws, for the location of the 1-bar-pressure surface $\mathcal{S}_{\rm o}$, and for the location of the three interfaces $\mathcal{S}_{\rm c}$, $\mathcal{S}_{\rm t}$ and $\mathcal{S}_{\rm m}$, Equations (5)–(7) can be solved via an iterative scheme on a massively parallel computer. The final hydrostatic equilibrium solution – which satisfies both Equations (5)–(7) and boundary conditions (8)–(9) and is constrained by the three gravitational coefficients, $J_{2n}, n = 1, 2, 3$ – results in the core density $\rho_{\rm c}$, the shape $\mathcal{S}_{\rm c}$ of the ice-rock core, the location and shape of the interfaces $\mathcal{S}_{\rm c}$, $\mathcal{S}_{\rm t}$ and $\mathcal{S}_{\rm m}$,

the properties of the thin metallic–molecular transition layer, the shape of the 1-bar pressure surface $\mathcal{S}_{\rm o}$ and the internal density and pressure distribution, $\rho(\boldsymbol{r})$ and $p(\boldsymbol{r})$ respectively, in the fluid region $\mathcal{D}_{\rm o}$.

The interior structure of Saturn resulting from our self-consistent model is summarized in Figure 2. It is found that the shape of the core-metallic interface $\mathcal{S}_{\rm c}$ can be accurately approximated by the oblate spheroid

$$\frac{x^2+y^2}{R_{\rm c}^2}+\frac{z^2}{R_{\rm c}^2(1-\mathcal{E}_{\rm c}^2)}=1,$$

where the eccentricity $\mathcal{E}_{\rm c}=0.2113$ and the core equatorial radius $R_{\rm c}=0.2031\,R_{\rm S}$. Our exact Saturnian model yields the core density $\rho_{\rm c}=10388.1\,{\rm kg\,m^{-3}}$ corresponding to the core mass $M_{\rm c}=13.06$ Earth masses, which is largely consistent with existing interior models of Saturn (Stevenson 1982; Guillot 2005). Furthermore, our model reveals that the 1-bar pressure surface $\mathcal{S}_{\rm o}$ of Saturn, when the effect of its zonal winds is neglected, can be described by the following equation

$$\begin{aligned}\xi_{\text{1-bar surface}} =& 2.076130\times[1+4.956\times10^{-4}\tilde{P}_2(\eta)\\ &+1.8678\times10^{-3}\tilde{P}_4(\eta)\\ &-1.372\times10^{-4}\tilde{P}_6(\eta)\\ &+1.18\times10^{-5}\tilde{P}_8(\eta)+\cdots],\end{aligned}\tag{10}$$

where $\eta$ denotes the spheroidal radius in oblate spheroidal coordinates $(\xi,\eta,\phi)$ defined by

$$x = 26\,139\sqrt{(1+\xi^2)(1-\eta^2)}\cos\phi\ \ ({\rm km}),\tag{11}$$

$$y = 26\,139\sqrt{(1+\xi^2)(1-\eta^2)}\sin\phi\ \ ({\rm km}),\tag{12}$$

$$z = 26\,139\xi\eta\ \ ({\rm km}),\tag{13}$$

with $-1\le\eta\le1$, $0\le\phi<2\pi$, and $\widetilde{P}_l(\eta)$ denoting the Legendre polynomials normalized by

$$\int_{-1}^{1}|\widetilde{P}_l(\eta)|^2\,{\rm d}\eta=1.$$

For instance, we have

$$\tilde{P}_2(\eta) = \sqrt{\frac{5}{8}}(3\eta^2-1),$$

$$\tilde{P}_4(\eta) = \sqrt{\frac{9}{128}}(35\eta^4-30\eta^2+3).$$

Using Equation (10) together with Equations (11)–(13), we obtain the equatorial radius at the 1-bar pressure level, evaluated by letting $\eta=0$, $(R_{\rm S})_{\rm model}=60\,268\,{\rm km}$ while the polar radius, evaluated by letting $\eta=1$, is $(R_{\rm p})_{\rm model}=54\,364\,{\rm km}$, in agreement with the observed values given in Table 1. It should be reiterated that our model does not make the spheroidal-shape approximation and that the shape of the 1-bar pressure surface $\mathcal{S}_{\rm o}$ given in Equations (10) is non-spheroidal and irregular (because the coefficients for $\tilde{P}_{2n}(\eta), n=1,2,3,\cdots$ are non-zero). However, all the coefficients for $\tilde{P}_n(\eta)$ with $n\ge2$ in the expression in Equation (10) are $\mathrm{O}(10^{-3})$ or smaller. It follows that, although the shape of Saturn is irregular, its deviation from a perfect oblate spheroid is too small to be noticeable in any reasonable plots. This small deviation is consistent with other rapidly rotating giant planets (Kong et al. 2015).

Our Saturnian model also reveals that (i) the metallic–molecular transition takes place at $r_{\rm e}=0.6139\,R_{\rm S}$, where $r_{\rm e}$ denotes the radial distance in the equatorial plane; (ii) the values of $K$ and $n$ change slightly across the metallic–molecular transition layer: while $K_1=240274.5\,{\rm Pa\,m^6kg^{-2}}$ and $n_1=1.0572$ in the metallic region $0.2031R_{\rm S}<r_{\rm e}<0.6139\,R_{\rm S}$, they increase to $K_2=240332.9\,{\rm Pa\,m^6\,kg^{-2}}$ and $n_2=1.0673$ in the molecular region where $0.6641R_{\rm S}<r_{\rm e}<R_{\rm S}$, with its variation $\Delta K=58.4\,{\rm Pa\,m^6\,kg^{-2}}$ and $\Delta n=0.0101$ across the transition layer whose thickness is about $0.05\,R_{\rm S}\approx3000\,{\rm km}$ (the variation of $K$ as a function of $r$ in the equatorial plane is shown in Fig. 3); (iii) the density at the bottom of the metallic region is $2.5593\times10^3\,{\rm kg\,m^{-3}}$, which decreases to $0.9303\times10^3\,{\rm kg\,m^{-3}}$ at the surface $\mathcal{S}_{\rm t}$ and then further to $0.8016\times10^3\,{\rm kg\,m^{-3}}$ at the surface $\mathcal{S}_{\rm m}$ across the transition layer; (iv) the density on the 1-bar pressure level at the surface $\mathcal{S}_{\rm o}$ is $0.63591\,{\rm kg\,m^{-3}}$; (v) the Saturnian convective dynamo is likely to operate in the metallic region approximately defined by the equatorial radius $0.2\,R_{\rm S}<r_{\rm e}<0.7\,R_{\rm S}$; and (vi) the total mass of Saturn in our model can be computed according to the formula

$$\begin{aligned}(M_{\rm S})_{\rm model}=&\iiint_{\mathcal{D}_{\rm c}}\rho_{\rm c}\,{\rm d}^3\boldsymbol{r}'\\ &+\iiint_{\mathcal{D}_{\rm o}}\rho\,(\boldsymbol{r}')\,{\rm d}^3\boldsymbol{r}',\end{aligned}$$

$(M_{\rm S})_{\rm model}$ denotes Saturn's mass enclosed by the 1-bar pressure surface $\mathcal{S}_{\rm o}$, which gives $(M_{\rm S})_{\rm model}=5.6836\times10^{26}\,{\rm kg}$, in agreement with the known mass of Saturn listed in Table 1.

Figure 4 shows the density $\rho\,(\boldsymbol{r})$ and pressure $p\,(\boldsymbol{r})$ as a function of $r$ in the equatorial plane in the interior of Saturn computed from our model. The small variations of $K$ and $n$ across the metallic–molecular regions

**Table 1** The Four Parameters of Saturn that are Regarded as Accurately Determined by Existing Measurements

| | |
|---|---|
| $GM_{\rm S}$ | $3.7931 \times 10^{16}\,{\rm m^3\,s^{-2}}$ (Williams 2016) |
| Equatorial Radius ($R_{\rm S}$) | 60 268 km (Williams 2016) |
| Polar Radius ($R_{\rm p}$) | 54 364 km (Williams 2016) |
| $\Omega_{\rm S}$ | $1.65434 \times 10^{-4}\,{\rm s^{-1}}$ (Helled et al. 2015) |

Notes: $GM_{\rm S}$, equatorial radius $R_{\rm S}$, polar radius $R_{\rm p}$ and angular velocity $\Omega_{\rm S}$.

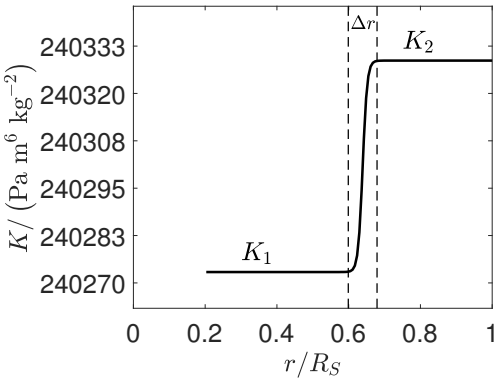


**Fig. 3** The value of $K$ for the polytropic law in the Saturnian fluid region $\mathcal{D}_{\rm o}$ as a function of $r$ in the equatorial plane, where the thickness of the transition layer is about $\Delta r = 0.05\,R_{\rm S} \approx 3000$ km.

shown in Figure 3 and the non-discontinuous profiles of the density and pressure shown in Figure 4 indicate that one simple polytropic EOS (Chandrasekhar 1933; Hubbard 1999; Horedt 2004) can be employed to model, to leading-order approximation, both the metallic and molecular regions of Saturn.

Our model yields the three known gravitational coefficients $J_2, J_4, J_6$ and predicts the three higher coefficients $J_8, J_{10}, J_{12}$ for Saturn in its hydrostatic state. After determining the core density $\rho_{\rm c}$ in $\mathcal{D}_{\rm c}$, the shape of the core-metallic interface $\mathcal{S}_{\rm c}$, the shape of the 1-bar pressure surface $\mathcal{S}_{\rm o}$ and the density profile $\rho(\boldsymbol{r})$ in the fluid region $\mathcal{D}_{\rm o}$, we can compute the external gravitational potential $V_{\rm g}(\boldsymbol{r})$ according to

$$V_{\rm g}(\boldsymbol{r}) = -G\left[\iiint_{\mathcal{D}_{\rm c}} \frac{\rho_{\rm c}{\rm d}^3\boldsymbol{r}'}{|\boldsymbol{r}-\boldsymbol{r}'|} + \iiint_{\mathcal{D}_{\rm o}} \frac{\rho\,(\boldsymbol{r}')\,{\rm d}^3\boldsymbol{r}'}{|\boldsymbol{r}-\boldsymbol{r}'|}\right],$$

where $|\boldsymbol{r}| \geq R_{\rm S}$, which is then further expanded in terms of the zonal gravitational coefficients $J_{2n}$

$$V_{\rm g}(\boldsymbol{r}) = -\frac{GM_{\rm S}}{r}\left[1 - \sum_{n=2}^{\infty} J_{2n}\left(\frac{R_{\rm S}}{r}\right)^{2n} P_{2n}(\cos\theta)\right], \quad r > R_{\rm S}, \tag{14}$$

where the coefficients $J_{2n}$ are computed as

$$\begin{aligned} J_n = &-\frac{(4n+1)R_{\rm S}}{2M_{\rm S}} \times \int_0^{\pi}\left[\iiint_{\mathcal{D}_{\rm c}} \frac{\rho_{\rm c}{\rm d}^3\boldsymbol{r}'}{|\boldsymbol{r}-\boldsymbol{r}'|}\right. \\ &\left. + \iiint_{\mathcal{D}_{\rm o}} \frac{\rho\,(\boldsymbol{r}')\,{\rm d}^3\boldsymbol{r}'}{|\boldsymbol{r}-\boldsymbol{r}'|}\right]_{|\boldsymbol{r}|=R_{\rm S}} \\ &\times \sin\theta P_{2n}(\cos\theta)\,{\rm d}\theta. \end{aligned} \tag{15}$$

Values of the zonal gravitational coefficients $J_n$, up to $n = 12$, computed from the exact solution through Equations (15), are listed in the second column of Table 2. It can be seen that the low-order gravitational coefficients $J_2, J_4$ and $J_6$ from our model agree with the three known coefficients (the third column of Table 2) of Saturn (Helled et al. 2015) within their error bars. Table 2 also provides the predicted values of the higher-order coefficients, $J_8, J_{10}$ and $J_{12}$, based on our Saturnian model.

## 4 SUMMARY AND REMARKS

We have presented the first self-consistent, exact interior model of Saturn that consists of an ice-rock core, a metallic region, an outer molecular envelope and a thin transition layer between the metallic and molecular regions. Constrained by the known mass, the known equatorial and polar radii, and the known low-order gravitational coefficients, $J_{2n}, n = 1, 2, 3$, of Saturn, the model determines an ice-rock core with the equatorial radius

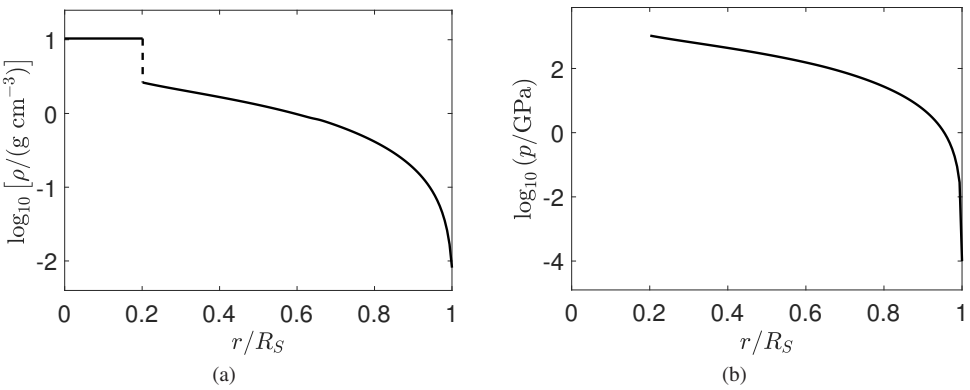


**Fig. 4** The interior structure of Saturn resulting from the fully self-consistent model: (a) the density $\rho$ as a function of $r/R_{\rm S}$ in the equatorial plane and (b) the pressure $p$ as a function of $r$ in the equatorial plane.

**Table 2** The Lower-order Gravitational Zonal Coefficients

| | Exact model | Observation (Helled et al. 2015) |
|---|---|---|
| $J_2 \times 10^6$ | $+16290.76$ | $+16290.71 \pm 0.27$ |
| $J_4 \times 10^6$ | $-935.67$ | $-935.83 \pm 2.77$ |
| $J_6 \times 10^6$ | $+83.22$ | $+86.14 \pm 9.64$ |
| $J_8 \times 10^6$ | $-9.40$ | – |
| $J_{10} \times 10^6$ | $+1.23$ | – |
| $J_{12} \times 10^6$ | $-0.18$ | – |

Notes: $J_2, J_4, J_6$ in the expansion in Eq. (14) obtained from our exact Saturnian model compared with the observed values (Helled et al. 2015) and the predicted values of the higher-order coefficients, $J_8, J_{10}$ and $J_{12}$ based on our exact model.

$0.203\,R_{\rm S}$ corresponding to 13.06 Earth masses, produces the hydrostatic shape of Saturn at the 1-bar pressure given by expression Equation (10), predicts the values of the higher-order gravitational coefficients $J_8, J_{10}, J_{12}$ presented in Table 2, and suggests that the Saturnian dynamo operates in the metallic region approximately defined by $0.2\,R_{\rm S} < r < 0.7\,R_{\rm S}$. Note that the Saturnian shape at the 1-bar pressure level given by Equation (10) is geometrically irregular and determined self-consistently and exactly by the required equilibrium conditions.

This paper is the first in a series on the gravitational field, shape and zonal winds of Saturn. We have avoided an important question in the present study: if the zonal winds on Saturn are sufficiently deep and strong, the density anomaly in the deep interior of the planet induced by the winds can slightly alter the zonal gravitational coefficients in Table 2, particularly the values of higher-order coefficients such as $J_{10}$ and $J_{12}$ (see, for example, Hubbard 1999; Kong et al. 2015). This is because both the rotational distortion and the equatorially symmetric zonal winds can make contributions to the even coefficients $J_{2n}$. In the second paper of this series (Kong et al. 2018), we will study how the structure and amplitude of the equatorially symmetric fluid motion in the deep interior of Saturn can affect its gravitational field and we will adopt a self-consistent perturbation approach (Zhang et al. 2017) in that the variation of the gravitational field is caused solely by the effect of the equatorially symmetric zonal winds on the rotationally distorted non-spheroidal Saturn. In other words, variations in the high-order gravitational coefficients provide a way of probing or constraining the internal structure of the zonal winds on Saturn.

The irregular hydrostatic shape of the 1-bar pressure surface $\mathcal{S}_{\rm o}$ described by Equation (10) may be slightly different from the actually measured shape of Saturn. This is because the zonal winds with a typical speed $\mathrm{O}(100)\,\mathrm{m\,s^{-1}}$ on a giant planet, if they are sufficiently deep, would alter the hydrostatic shape about $\mathrm{O}(10)\,\mathrm{km}$ (for example, Kong et al. 2012). This implies that some uncertainties might exist in the size of the equatorial radius $R_{\rm S}$ adopted in our Saturnian model, but uncer-

tainties in the polar radius $R_{\rm p}$ would be much smaller. Finally, we note that possible tidal effects in connection with the moons of a giant planet (see, for example, Ogilvie 2013; Chen 2003) are completely neglected in the present model.

**Acknowledgements** KZ is supported by Leverhulme Trust Research Project Grant RPG-2015-096, by STFC Grant ST/R000891/1 and by Macau FDCT grants 007/2016/A1 and 001/2016/AFJ. DK is supported by 1000 Youth Talents Programme of China. The computation made use of the high performance computing resources in the Core Facility for Advanced Research Computing at SHAO, CAS.

## References

Anderson, J. D., & Schubert, G. 2007, Science, 317, 1384
Cao, H., & Stevenson, D. J. 2017, Journal of Geophysical Research (Planets), 122, 686
Chandrasekhar, S. 1933, MNRAS, 93, 390
Chen, C. X. 2003, Journal of Geophysical Research (Space Physics), 108, 1376
Guillot, T. 2005, Annual Review of Earth and Planetary Sciences, 33, 493
Helled, R., Galanti, E., & Kaspi, Y. 2015, Nature, 520, 202
Horedt, G. P., ed. 2004, Astrophysics and Space Science Library, 306, Polytropes - Applications in Astrophysics and Related Fields
Hubbard, W. B. 1973, Annual Review of Earth and Planetary Sciences, 1, 85
Hubbard, W. B. 1999, Icarus, 137, 357
Kong, D., Zhang, K., & Schubert, G. 2012, ApJ, 748, 143
Kong, D., Zhang, K., Schubert, G., & Anderson, J. 2013, ApJ, 763, 116
Kong, D., Zhang, K., & Schubert, G. 2015, Physics of the Earth and Planetary Interiors, 249, 43
Kong, D., Zhang, K., & Schubert, G. 2016, ApJ, 826, 127
Kong, D., Zhang, K., Schubert, G., & Anderson, J. 2018, RAA (Research in Astronomy and Astrophysics), 18, 39
Militzer, B. 2013, Phys. Rev. B, 87, 014202
Ogilvie, G. I. 2013, MNRAS, 429, 613
Read, P. L., Dowling, T. E., & Schubert, G. 2009, Nature, 460, 608
Saumon, D., Chabrier, G., & van Horn, H. M. 1995, ApJS, 99, 713
Seidelmann, P. K., Archinal, B. A., A'Hearn, M. F., et al. 2007, Celestial Mechanics and Dynamical Astronomy, 98, 155
Smith, B. A., Soderblom, L., Batson, R. M., et al. 1982, Science, 215, 504
Stevenson, D. J. 1982, Annual Review of Earth and Planetary Sciences, 10, 257
Williams, D. R. 2016, Saturn Fact Sheet, *https://nssdc.gsfc.nasa.gov/planetary/factsheet/saturnfact.html*
Zhang, K., Kong, D., & Schubert, G. 2017, Annual Review of Earth and Planetary Sciences, 45, 419
Zharkov, V. N., & Trubitsyn, V. P. 1978, Physics of planetary interiors (Tucson: Pachart)